

# Synthesis and Liquid Crystalline Properties of Unsymmetrically Substituted Naphthalenediimides with a Polar Headgroup: Effect of Amide Hydrogen Bonding and Alkyl Chain Length

Namdev V. Ghule,<sup>[a]</sup> Rajesh S. Bhosale,<sup>[a]</sup> Sidhanath V. Bhosale,<sup>\*,[a]</sup> Turlapati Srikanth,<sup>[b]</sup> Nandiraju V. S. Rao,<sup>\*,[b]</sup> and Sheshanath V. Bhosale<sup>\*,[c]</sup>

A series of new unsymmetrically substituted naphthalenediimide (NDI) moieties **NDI-1** to **NDI-6** were synthesized. The structures of these compounds were confirmed by means of FT-IR, <sup>1</sup>H NMR, <sup>13</sup>C NMR, ESI-mass and HRMS spectroscopic measurements. UV/Vis and fluorescence spectroscopy were employed to investigate the photophysical properties of the prepared compounds in solution and in the solid state. Using the onset of UV/Vis absorption, the optical band gaps were calculated. Cyclic voltammetry measurements were performed

to study the electrochemical behavior and to calculate the LUMO energy levels. The thermal properties of NDI derivatives were studied by differential scanning calorimetry. The mesomorphic birefringent behavior of the NDI derivatives was investigated with polarizing optical microscopy. Among all of the studied NDI derivatives, only **NDI-1**, **NDI-2**, and **NDI-3** showed liquid crystalline texture, owing to the presence of an amide linkage for H-bonding along with aromatic moieties for  $\pi$ - $\pi$ -stacking.

## 1. Introduction

The design, synthesis, and optical properties of organic  $\pi$ -conjugated systems are studied in different fields, which have attracted considerable attention from various research groups in recent years. The self-assembled and self-organized  $\pi$ -conjugated systems possess excellent potential to be employed in organic semiconductor devices and charge-transporting devices. Furthermore, their ability to exhibit liquid crystalline (LC) behavior is very interesting.<sup>[1–3]</sup> During the synthesis of LC materials, researchers were troubled by the solubility issue with higher molecular analogues. Hence, researchers turned their

attention towards lower-molecular-weight analogue derivatives to overcome the solubility issue and succeeded to realize the LC behavior. Liquid crystallinity is the fourth state of matter, that is, an intermediate state between solid crystals and conventional liquid, and is distinguished by different molecular orientations, alignments, and ordered states.

LC materials are electrical insulators and are employed in flat panel displays and for developing semiconductor materials.<sup>[4]</sup> Mostly,  $\pi$ -conjugated systems have been used during the construction of LC materials, because it assists in inducing  $\pi$ - $\pi$  stacking and hydrogen-bonding interactions to promote self-assembly and self-organization. Whereas the self-organization asserts aggregation and exhibits appropriate orientations for LC materials, the polar headgroups also play a vital role during the alignment of LC materials, not only for thermotropic, but also for lyotropic LC phases.<sup>[5]</sup>

Naphthalenediimide (NDI) and its derivatives are excellent *n*-type semiconductor materials with high electron affinities, owing to their self-organization manifested by the  $\pi$ - $\pi$  stacking.<sup>[6,7]</sup> NDI is an ideal building block for the construction of self-assembled nanostructures such as nanowires, nanoflowers, nanosheets, vesicles, nanospheres, golf-ball-like morphology, nanotubes, nanowires, rods, and ribbons because of their high  $\pi$ - $\pi$  stacking interactions.<sup>[8–18]</sup> Nevertheless, NDIs are lower homologues among other rylene diimides and have been studied extensively in the field of optoelectronics, fabrication of field-effect transistors, organic light-emitting diodes, and flexible LC display, owing to charge carrier mobility and  $\pi$ -electron delocalization, which leads to conductivity.<sup>[19–24]</sup> Yitzchaik and co-workers<sup>[25]</sup> first studied the molecular layer epitaxy of NDI de-

[a] N. V. Ghule, Dr. R. S. Bhosale, Dr. S. V. Bhosale  
Polymers and Functional Materials Division  
CSIR-Indian Institute of Chemical Technology  
Hyderabad 500007, Telangana (India)  
E-mail: bhosale@iict.res.in

[b] Dr. T. Srikanth, Prof. Dr. N. V. S. Rao  
Chemistry Department, Assam University  
Silchar 788011, Assam (India)  
E-mail: nandirajuv@gmail.com

[c] Dr. S. V. Bhosale  
School of Science, RMIT University  
GPO Box 2476V, Melbourne, VIC-3001 (Australia)  
E-mail: bsheshanath@gmail.com

Supporting Information and the ORCID identification number(s) for this author(s) of this article can be found under <https://doi.org/10.1002/open.201700151>.

© 2017 The Authors. Published by Wiley-VCH Verlag GmbH & Co. KGaA. This is an open access article under the terms of the Creative Commons Attribution-NonCommercial-NoDerivs License, which permits use and distribution in any medium, provided the original work is properly cited, the use is non-commercial and no modifications or adaptations are made.

derivatives and LC properties. Schab-Balcerzak et al. reported the synthesis and thermotropic LC properties of azomethine–NDI for optoelectronic applications.<sup>[26]</sup> Reckzek and co-workers established the charge transfer in columnar LC materials using NDI (acceptor) and alkoxy anthracene (donor).<sup>[27]</sup> Recently, Xiao et al. demonstrated LC properties of NDI-based dyads, triads with a substituted triphenylene core as the donor.<sup>[28]</sup>

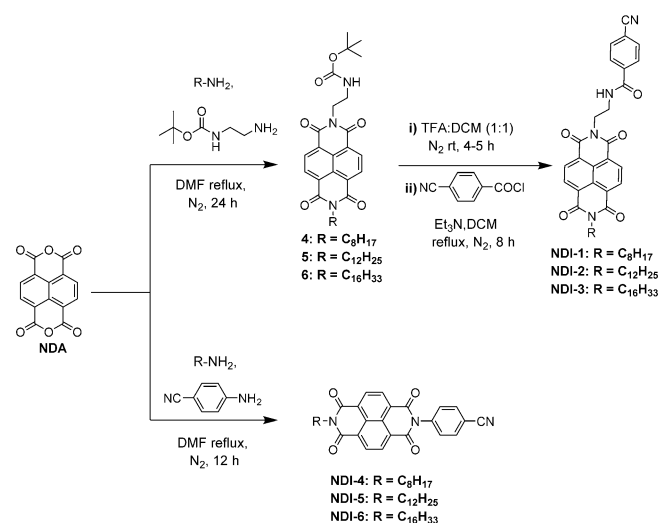
The changes in alkyl chain length are well documented to affect the aggregation ability, thermal, and electronic properties of the material.<sup>[29]</sup> Furthermore, Lee et al. demonstrated that, by tuning the alkyl chain length of the NDI polymer, the electron mobility and solar cell efficiency in organic photovoltaics are enhanced.<sup>[30]</sup>

The above comprehensive list of applications of NDI, including the donor–acceptor motif, motivated us to design and synthesize unsymmetrical NDI derivatives with alkyl chains at one end and a cyanophenyl moiety at the other terminal end. Herein, we report the synthesis of NDI derivatives **NDI-1** to **NDI-6**, and demonstrated the distinct influence of an amide linkage and long alkyl chains to manifest the LC properties. The  $\pi$ – $\pi$  stacking and amide hydrogen bonding would assist for self-organization and a polar headgroup such as a nitrile would be beneficial, which takes part in enhancing the dipole moment and assigns appropriate orientations in the liquid crystal.<sup>[31]</sup>

## 2. Results and Discussion

### 2.1. Synthesis and Characterization

The synthetic details for compounds **NDI-1** to **NDI-3** are shown in Scheme 1. A one-step imide formation reaction between 1,4,5,8-naphthalene tetracarboxylic dianhydride (NDA), aliphatic amines, and monoboc ethylenediamine in dry dimethylformamide (DMF) yields compounds **4–6**. Compounds **4–6** were readily subjected to boc deprotection in the presence of 1:1 trifluoroacetic acid (TFA)/dichloromethane (DCM) to yield



Scheme 1. Synthetic scheme of **NDI-1** to **NDI-6** compounds.

the appropriate amines. These amines were further used for coupling with the acid chloride of 4-cyano benzoic acid in the presence of triethylamine/DCM to give the desired products **NDI-1** to **NDI-3**. Furthermore, all compounds were fully characterized by using spectroscopic techniques. Furthermore, **NDI-4** to **NDI-6** were prepared via imide formation reaction by using NDA, alkyl amine, and 4-amino benzonitrile, as outlined in Scheme 1. Similarly, the chemical structures of **NDI-4** to **NDI-6** were also confirmed by spectral and elemental analysis.

The obtained analytical data of **NDI-1** are in good agreement with their chemical structure. The <sup>1</sup>H NMR spectrum of compound **NDI-1** is discussed; a peak for four protons of the NDI core appeared as a singlet at 8.85–8.81 ppm. The nitrile-bearing phenyl ring exhibits one singlet peak for four protons at 7.80 ppm. The amide proton peak was observed at 7.64–7.62 ppm as a broad singlet. In the <sup>13</sup>C NMR spectrum, the characteristic peak of –CN carbon appeared at  $\delta$  115.61 ppm. The obtained HRMS value, 551.2289, confirms the structure of compound **NDI-1**. The FT-IR peaks at 1658 and 1702 cm<sup>-1</sup> of **NDI-1** confirmed the presence of amide and imide carbonyl functional groups, respectively, along with the –CN stretching peak at 2231 cm<sup>-1</sup>. In compounds **NDI-2** to **NDI-6**, the elemental analysis deviation for carbon, hydrogen, and nitrogen was found to be more than 0.3%, which could be attributed to the presence of solvent trapped in the LC compounds. Usually, it is very difficult to remove the trapped solvent from such  $\pi$ -conjugated small molecules.

The synthesized compounds were further characterized by using UV/Vis and fluorescence spectroscopy techniques.

### 2.2. UV/Vis and Fluorescence Study

UV/Vis absorption and emission spectroscopy were employed to study the photophysical properties of **NDI-1** to **NDI-6**. The UV/Vis absorption spectra were measured both in tetrahydrofuran (THF) solution and in a thin film coated onto a glass substrate (Figure 1). Absorption spectra of **NDI-1** to **NDI-6** showed two intense peaks at 358 and 378 nm along with one shoulder

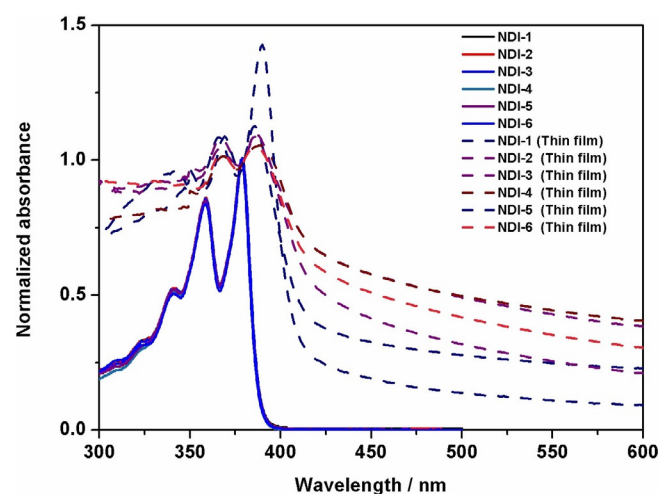


Figure 1. Normalized UV/Vis spectra of **NDI-1** to **NDI-6** in  $1 \times 10^{-5}$  M THF solution (solid lines) and thin films (dashed line).

peak at 340 nm. The absorption peaks above 340 nm are characteristic peaks for NDIs and attributes the  $\pi-\pi^*$  transition. Significant redshifts in the absorption peaks of thin films of these synthesized NDIs are observed with respect to all NDIs in solution, reflecting the conformations of  $\pi-\pi$  stacking and aggregation. The photophysical data of **NDI-1** to **NDI-6** are detailed in Table 1.

Compound	$\lambda_{\max}$ (abs) [nm]	$\epsilon$ [ $L M^{-1} cm^{-1}$ ]	$\lambda_{\max}$ (em) [nm]	UV/Vis (film) [nm]	$\epsilon$ [ $L M^{-1} cm^{-1}$ ]
<b>NDI-1</b>	379	27 700	403	388	65553
<b>NDI-2</b>	379	13 400	401	388	34260
<b>NDI-3</b>	378	13 500	405	387	69478
<b>NDI-4</b>	379	34 700	401	387	89953
<b>NDI-5</b>	379	29 400	405	388	64948
<b>NDI-6</b>	379	19 700	403	388	97169

[a]  $\epsilon$  = Absorbance.

Upon excitation at 355 nm, compounds **NDI-1** to **NDI-6** shows emission peaks at 403, 401, 405, 401, 405, and 403 nm, respectively (Figure 2 and Table 1). The thin film fluorescence

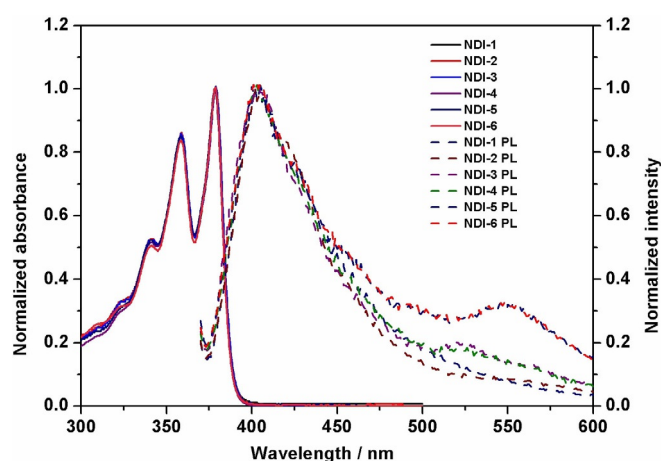


Figure 2. Normalized UV/Vis spectra (solid line) of **NDI-1** to **NDI-6** and fluorescence emission ( $\lambda_{\text{ex}} = 355$  nm) spectra (dashed line) in THF ( $1 \times 10^{-5}$  M).

emission spectra were recorded on a quartz substrate with excitation at 355 nm; it can be clearly seen that the 403, 401, and 405 nm peaks for **NDI-1** to **NDI-3** are present, with additional broad emission peaks at 530, 528, and 550 nm, respectively (Figure S1). However, for **NDI-4** to **NDI-6**, the additional emission peaks appeared at 455, 460, and 462 nm, respectively (Figure S1). The appearance of additional emission peaks could be attributed to the  $\pi-\pi$  stacking of the NDI core in the solid state. Nevertheless, the appearance of pronounced redshifts in emission peaks of **NDI-1** to **NDI-3** compared to **NDI-4** to **NDI-6** are attributed to  $\pi-\pi$  stacking of the NDI core along with the presence of amide hydrogen-bonding interactions in thin film.

## 2.3. Electrochemical Properties

The electrochemical properties of **NDI-1** to **NDI-6** were measured by using cyclic voltammetry (CV). The obtained voltammograms of the NDI derivatives are presented in Figure 3. The

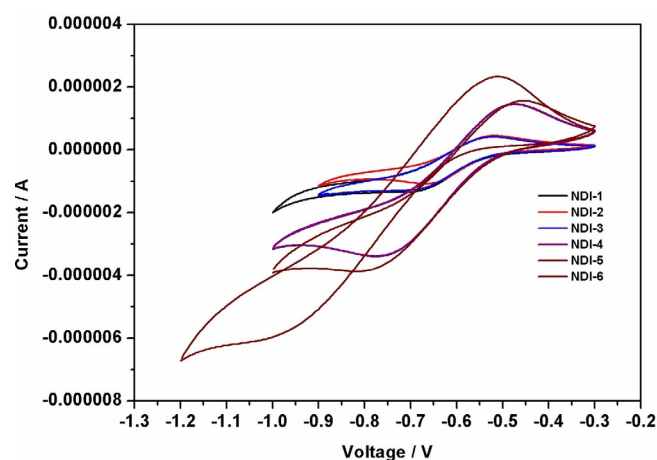


Figure 3. Overlapped cyclic voltammograms of **NDI-1** to **NDI-6** in THF ( $1 \times 10^{-5}$  M) with a scan rate of  $50 \text{ mV s}^{-1}$ ,  $0.1 \text{ M Bu}_4\text{VClO}_4$  supporting electrolyte, a Pt disk working electrode, a Pt wire counter electrode, and a saturated calomel reference electrode.

**NDI-1** to **NDI-6** compounds exhibited a single electrochemical reduction process characteristic of NDI between potentials of  $-0.7$  and  $-0.6$  V. Determination of onset reduction potential values allowed the calculation of the lowest unoccupied molecular orbital (LUMO). The optical band gap values ( $E_g \approx 3.17$  to  $3.18$  eV) for the NDI derivatives were calculated from the onset of the UV/Vis absorption band, as enlisted in Table 2. Utilizing the LUMO values and optical band gap, we determined the HOMO values of **NDI-1** to **NDI-6**.

Compound	$\lambda_{(\text{onset})}$ [nm]	$E_g = 1240/\lambda_{(\text{onset})}$ [nm]	$E_{(\text{onset, red})}$ [V]	LUMO [eV] <sup>[a]</sup>	HOMO [eV] <sup>[b]</sup>
<b>NDI-1</b>	389	3.18	$-0.75$	$-4.05$	$-7.23$
<b>NDI-2</b>	389	3.17	$-0.67$	$-4.13$	$-7.30$
<b>NDI-3</b>	390	3.18	$-0.78$	$-4.02$	$-7.20$
<b>NDI-4</b>	390	3.17	$-0.96$	$-3.84$	$-7.01$
<b>NDI-5</b>	389	3.18	$-0.67$	$-4.13$	$-7.31$
<b>NDI-6</b>	389	3.18	$-0.64$	$-4.16$	$-7.34$

[a] LUMO [eV] =  $-[E_{\text{red}} + 4.8]$ . [b] HOMO [eV] = LUMO -  $E_g$

## 2.4. Phase Behavior and LC Properties

### 2.4.1. Differential Scanning Calorimetry (DSC) Measurements

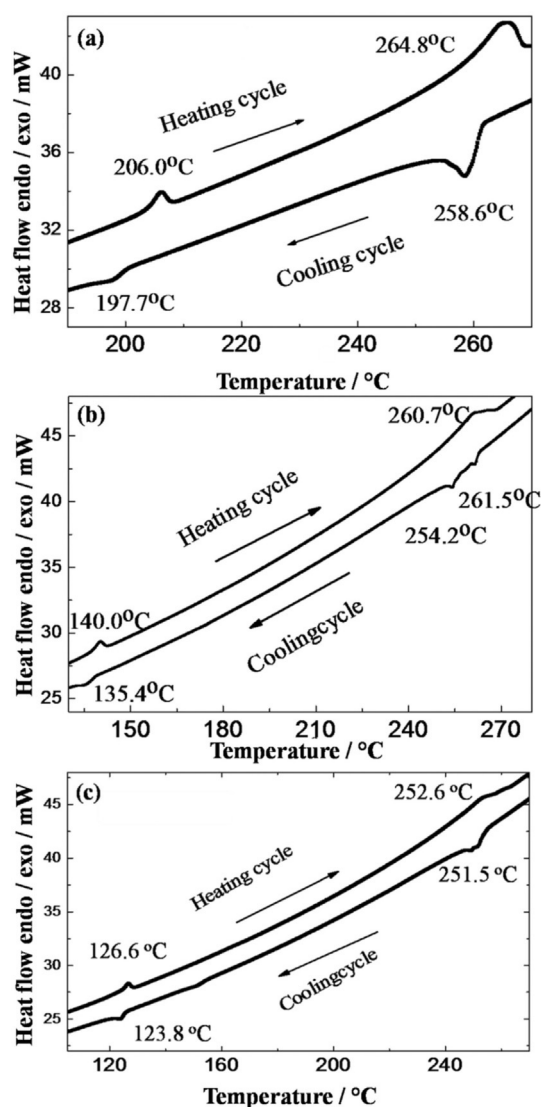
The thermal properties of the compounds show multiple transitions, as estimated by DSC during heating and cooling cycles. Mostly, on the second heating cycle, the phase transitions disappeared, which could be assigned to the melting of crystals,<sup>[32]</sup> whereas the second cooling cycle assigns the molten

**Table 3.** Phase-transition temperatures of compounds **NDI-1** to **NDI-6**, recorded for the second heating cycle (first row) and second cooling cycle (second row) at  $5^{\circ}\text{C min}^{-1}$  from DSC and confirmed with POM. The enthalpies ( $\Delta H$  in  $\text{kJ mol}^{-1}$ ) and entropies ( $\Delta S$  in  $\text{J m}^{-1}$ ) are presented in parentheses.

Crystalline Compound	Liquid crystalline		Isotropic	
	Heating [ $^{\circ}\text{C}$ ]	Cooling [ $^{\circ}\text{C}$ ]	Heating [ $^{\circ}\text{C}$ ]	Cooling [ $^{\circ}\text{C}$ ]
NDI-1	206.0 (3.06, 6.39)	197.7 (2.27, 4.82)	264.8 (22.8, 42.4)	258.6 (21.9, 41.1)
NDI-2	140.0 (2.97, 7.20)	135.4 (2.79, 6.84)	260.7 (15.5, 29.2)	254.2 (3.0, 5.73) LC1 261.5 (0.66, 1.23)
NDI-3	126.6 (2.17, 5.46)	123.8 (3.59, 9.06)	252.6 (6.61, 15.2)	251.5 (9.40, 17.9)
NDI-4			287.1 (36.0, 64.2)	260.8 (38.7, 72.7)
NDI-5			285.1/273.1	
NDI-6	140.7 (5.47, 10.6)	139.1 (6.89, 13.4)	262.5 (30.3, 56.7)	256.6 (29.8, 56.3)

phase of the liquid. The second heating and first cooling DSC thermograms at  $10^{\circ}\text{C min}^{-1}$  were recorded and the results are presented in Table 3. The DSC thermograms include the series of synthesized unsymmetrical NDI derivatives **NDI-1** to **NDI-6**. NDI derivatives **NDI-1** to **NDI-3** bearing an amide linkage show

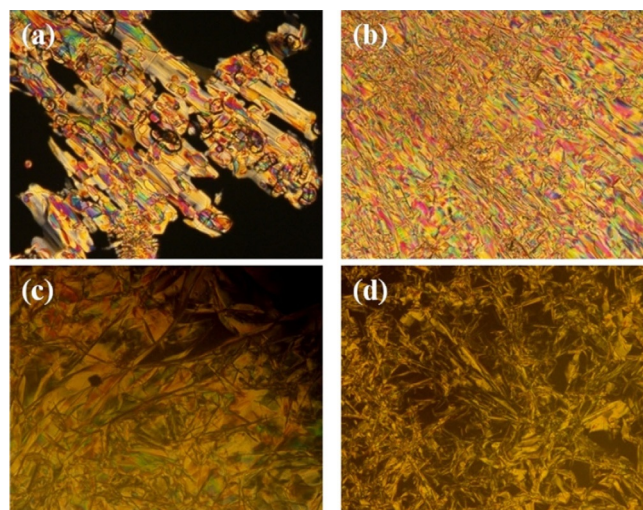
the transition phase at different temperatures, which is shown in Figure 4. In **NDI-4** to **NDI-6**, such behavior is not observed (Figure S2).

**Figure 4.** DSC thermograms of model compounds: a) **NDI-1**, b) **NDI-2**, and c) **NDI-3** recorded at a heating/cooling rate of  $5^{\circ}\text{C min}^{-1}$ .

#### 2.4.2. Polarized Optical Microscopy (POM)

Compounds **NDI-1** to **NDI-3** were studied for their mesomorphic properties through the observation of optical textures with POM. Upon slow cooling, compound **NDI-1** exhibited a birefringent texture at  $258^{\circ}\text{C}$  (Table 3), which stabilized later with a consistent pattern and developed throughout the entire region of thin film. The texture resembles the textures observed for a discotic nematic phase, as shown in Figures 5a and 5b). The sample crystallized at  $198^{\circ}\text{C}$  (Table 3). Similarly, compound **NDI-2** exhibited a birefringent optical texture in the cooling cycle at  $254^{\circ}\text{C}$  (Table 3), as shown in Figure 5c. **NDI-3** also exhibited the LC texture at temperatures below  $251^{\circ}\text{C}$  (Table 3), as shown in Figure 5d.

As the alkyl chain length increases from  $\text{C}_8$  to  $\text{C}_{12}$  and  $\text{C}_{16}$ , the transition temperature decreases from  $258$  to  $254$  and  $251^{\circ}\text{C}$ , and the NDI derivatives exhibit a discotic nematic phase, birefringent, and crystalline phase, respectively. These

**Figure 5.** POM images of NDI derivatives: a) growth of mesomorphic birefringent texture at  $257^{\circ}\text{C}$  of **NDI-1**; b) fully developed birefringent texture  $256.7^{\circ}\text{C}$ ; c) mesomorphic texture of **NDI-2** at  $260^{\circ}\text{C}$ . d) Indicates mesomorphic texture of **NDI-3** at  $260^{\circ}\text{C}$ .

results suggest the change in alkyl chain length could change the LC phase with the respective transition temperature. Hence, it is concluded that the nature of the LC texture depends on the flexibility of the spacer, the linkage group, and the polar end group, which creates the transverse dipole moment that supports molecular interactions.<sup>[31]</sup> The LC properties were disrupted in the presence of an increasing percentage of amide linkages.<sup>[33]</sup> However, without an amide linkage, the NDI derivatives did not exhibit multiple phase transitions during the heating and cooling cycles. It implies that **NDI-4** to **NDI-6** (Figure S3) could not exhibit LC behavior, and we assume that the spacer as well as the type of linkage for molecular interactions plays an important role in inducing mesomorphism.

### 3. Conclusions

We have studied the effect of the amide linkage and different alkyl chain lengths on the liquid crystalline (LC) properties of NDI-based derivatives. In **NDI-1** to **NDI-3**, as the alkyl chain length increases from C<sub>8</sub> to C<sub>12</sub> and C<sub>16</sub>, it was observed that the transition temperature decreases from 258 to 254 and 251 °C, and different LC properties are observed, going from a discotic nematic phase to a birefringent and crystalline phase, respectively. Whereas, **NDI-4** to **NDI-6**, without a spacer or amide linkage, do not display any LC properties. These results imply the importance of the alkyl chain length as well as the amide linkage for hydrogen bonding in LC behavior. We believe that such an LC materials may have future potential applications in display devices such as TVs, mobile phones, computer monitors, and so forth.

## Experimental Section

1,4,5,8-Naphthalenetetracarboxylic dianhydride, aliphatic amines, and ethylenediamine were purchased from Sigma Aldrich (Bengaluru, Karnataka, India); 4-amino benzonitrile and 4-cyano benzoic acid were purchased from Spectrochem (Hyderabad, Telangana, India) and were used without further purification. Furthermore, all other solvents and chemicals were distilled and dried before use such as DMF, DCM, and triethylamine. Spectroscopic-grade solvents were used for all optical measurements.

### Spectroscopic Measurements

<sup>1</sup>H NMR spectra were recorded on AVANCE 300 and 500 MHz instruments. <sup>13</sup>C NMR spectra were recorded on 75, 100, and 125 MHz NMR spectrometers, using tetramethylsilane (TMS) as the internal standard and CDCl<sub>3</sub>-d<sub>1</sub> or [D<sub>6</sub>]DMSO as the solvent. Mass spectrometric data were obtained by using the positive electron spray ionization (ESI-MS) technique on an Agilent Technologies 1100 Series (Agilent Chemstation Software) mass spectrometer. High-resolution mass spectra (HRMS) were obtained by using an ESI-QTOF mass spectrometer. FT-IR spectra were recorded on a PerkinElmer spectrum-100 spectrometer. Elemental analysis was carried out by using a Vario Micro Cube.

### Optical Measurements

Electronic absorption and emission spectra were recorded on an Agilent Technologies Cary 5000 eclipse UV/Vis-NIR spectrophotometer and Agilent technologies Cary eclipse fluorescence spectrophotometer, respectively. For DSC, the phase transition temperatures and associated enthalpies were measured on a PerkinElmer Pyris-1 system with a heating/cooling rate of 5 °C min<sup>-1</sup>.

### Synthetic Procedures

#### Synthesis of Compound 4–6

In the synthesis of compounds **4**, **5**, and **6**, imidation reactions were performed by modifying a reported procedure.<sup>[16]</sup> 1,4,5,8-Naphthalenetetracarboxylic dianhydride (NDA) (1 g, 0.0037 mol) and mono boc-ethylene diamine (1.2 equiv) were mixed in 15 mL of dry DMF under a N<sub>2</sub> atmosphere, and then the reaction mixture was heated under reflux to yield a clear brown solution. Then, the aliphatic amine (1 equiv) was added into the reaction mixture. Furthermore, the reaction mixture was heated under reflux for 16 h in a N<sub>2</sub> atmosphere. The completion of the reaction was monitored by TLC analysis. After completion of reaction, the reaction mixture was cooled to room temperature. The solvent was removed under reduced pressure by using a rotary evaporator, which gave the crude product as a brown solid. This was re-precipitated by using methanol and removal of the solvent was subsequently achieved by filtration. The obtained product, a faint brown solid, was purified by column chromatography using silica gel (60–120 mesh), eluting with a mixture of DCM and hexane (8:2, v/v), followed by evaporation of solvent on a rotary evaporator under vacuum to yield the pure product as a brown solid (0.92 g, 48%).

Compounds **5** and **6** were synthesized by following the procedure adopted for synthesis of compound **4**.

#### Spectroscopic Data of Compound 4

FT-IR (KBr, cm<sup>-1</sup>): 3352, 2924, 1704, 1686, 1656; <sup>1</sup>H NMR (500 MHz, CDCl<sub>3</sub>, TMS) δ ppm: 8.77–8.74 (m, 4H, *J* = 7.6 Hz), 4.87 (br, 1H), 4.39–4.37 (t, 2H, *J* = 5.64 Hz), 4.20–4.17 (t, 2H, *J* = 7.26 Hz), 3.56–3.55 (t, 2H), 1.77–1.71 (m, 2H), 1.30–1.25 (m, 19H) 0.89–0.86 (t, 3H, *J* = 6.7 Hz); <sup>13</sup>C NMR (125 MHz, CDCl<sub>3</sub>, TMS) δ ppm: 163.09, 162.66, 156.09, 130.96, 130.80, 126.58, 126.37, 79.22, 40.96, 40.60, 39.10, 31.74, 29.64, 29.22, 29.13, 28.11, 28.01, 27.04, 22.57, 14.03; ESI-MS *m/z* (%): 544 [M + Na]<sup>+</sup>; HRMS: Calculated. for C<sub>29</sub>H<sub>36</sub>N<sub>3</sub>O<sub>6</sub> [M+H]<sup>+</sup>: 522.2598; found: 522.2598, Calculated. for C<sub>29</sub>H<sub>35</sub>N<sub>3</sub>O<sub>6</sub>Na [M + Na]<sup>+</sup>: 544.2417; found: 544.2418.

#### Spectroscopic Data of Compound 5

FT-IR (KBr, cm<sup>-1</sup>): 2920, 1697, 1660; <sup>1</sup>H NMR (400 MHz, CDCl<sub>3</sub>, TMS) δ ppm: 8.76 (m, 4H), 4.86 (br, 1H), 4.40–4.37 (t, 2H, *J* = 5.38 Hz), 4.21–4.17 (t, 2H, *J* = 7.45 Hz), 3.56 (t, 2H), 1.78–1.70 (m, 2H), 1.25–1.22 (m, 27H), 0.89–0.85 (t, 3H, *J* = 6.62 Hz); <sup>13</sup>C NMR (100 MHz, CDCl<sub>3</sub>, TMS) δ ppm: 161.90, 161.47, 132.25, 131.90, 127.42, 125.58, 78.73, 41.91, 40.90, 38.76, 31.93, 29.63, 29.24, 27.92, 27.45, 22.68, 13.99. ESI-MS *m/z* (%): 610 [M + Na]<sup>+</sup>.

#### Spectroscopic Data of Compound 6

FT-IR (KBr, cm<sup>-1</sup>) (**6**): 3425, 2916, 1703, 1659; <sup>1</sup>H NMR (500 MHz, CDCl<sub>3</sub>, TMS) δ ppm: 8.77–8.74 (m, 4H, *J* = 7.6 Hz), 4.86 (br, 1H),

4.39–4.37 (t, 2H,  $J=5.64$  Hz), 4.20–4.17 (t, 2H,  $J=7.26$  Hz), 3.56–3.55 (t, 2H), 1.75–1.72 (m, 2H), 1.25 (m, 35H), 0.89–0.86 (t, 3H,  $J=7.1$  Hz);  $^{13}\text{C}$  NMR (100 MHz,  $\text{CDCl}_3$ , TMS)  $\delta$  ppm: 163.19, 162.76, 156.12, 131.03, 130.86, 126.74, 126.66, 79.28, 41.01, 40.61, 39.15, 31.90, 29.67, 29.33, 28.11, 27.07, 22.61, 14.11; ESI-MS  $m/z$  (%): 535  $[\text{M}+\text{H}]^+$ .

### Synthesis of NDI-1

After boc deprotection of compound 4, 5, or 6 using TFA/DCM (1:1) at room temperature for 4–5 h, it was immediately used for further reactions to synthesize compounds NDI-1 to NDI-3.

A catalytic amount of DMF was added to 4-cyano benzoic acid (0.05 g, 0.00034 mol) in a 50 mL round-bottom flask. Distilled thionyl chloride (3.5 mL, 0.047 mol) was added dropwise at 0 °C to the aforementioned solution. The reaction mixture was heated under reflux for 6 h. The excess of thionyl chloride was evaporated under vacuum by using a rotary evaporator under a  $\text{N}_2$  atmosphere. Deprotected amine was mixed in dry DCM, and then the mixture was added dropwise to the acid chloride solution. Then, triethylamine (0.5 mL) was added at once to a stirred mixture of amine and acid chloride. The reaction mixture was stirred vigorously for 30 min under a  $\text{N}_2$  atmosphere. Then, the reaction mixture was heated under reflux for 8 h. The completion of the reaction was monitored by TLC, following which the reaction mixture was cooled to room temperature. Evaporation of solvent under reduced pressure yields a white residue, which was washed with saturated  $\text{NaHCO}_3$  and extracted with  $\text{CH}_2\text{Cl}_2$  (2  $\times$  25 mL). The obtained crude product was purified by column chromatography using DCM/MeOH (98:2, v/v) as an eluent, yielding pure product NDI-1 (0.083 g, 64%) as a solid.

Compounds NDI-2 and NDI-3 were synthesized following the procedure for the synthesis of NDI-1.

### Spectroscopic Data of Compound NDI-1

MP: 262 °C; FT-IR (KBr,  $\text{cm}^{-1}$ ): 3279, 2923, 2231, 1702, and 1658;  $^1\text{H}$  NMR (500 MHz,  $\text{CDCl}_3$ , TMS)  $\delta$  ppm: 8.85–8.81 (m, 4H,  $J=7.62$  Hz), 7.80 (s, 4H), 7.64–7.62 (brs, 1H), 4.62–4.60 (t, 2H,  $J=5.18$  Hz), 4.23–4.20 (t, 2H,  $J=7.62$  Hz), 4.02–3.92 (t, 2H), 1.77–1.71 (m, 2H), 1.26 (m, 10H), 0.89–0.86 (t, 3H);  $^{13}\text{C}$  NMR (75 MHz,  $\text{CDCl}_3$ , TMS)  $\delta$  ppm: 164.07, 162.88, 136.85, 132.78, 131.64, 131.23, 127.69, 127.09, 126.77, 125.83, 115.61, 112.65, 41.29, 40.57, 39.84, 31.75, 29.13, 27.98, 27.01, 22.59, 14.02; ESI-MS  $m/z$  (%): 551  $[\text{M}+\text{H}]^+$ ; HRMS  $m/z$  (%): calc. for  $\text{C}_{32}\text{H}_{31}\text{N}_4\text{O}_5$ : 551.2300; found: 551.2289.

### Spectroscopic Data of Compound NDI-2

MP: 272 °C; FT-IR (KBr,  $\text{cm}^{-1}$ ): 3281, 2920, 2233, 1702, and 1657;  $^1\text{H}$  NMR (400 MHz,  $\text{CDCl}_3$ , TMS)  $\delta$  ppm: 8.85–8.81 (m, 4H,  $J=7.62$  Hz), 7.80 (s, 4H), 7.64–7.62 (brs, 1H), 4.62–4.60 (t, 2H,  $J=5.18$  Hz), 4.23–4.20 (t, 2H,  $J=7.62$  Hz), 4.01–3.99 (t, 2H), 1.77–1.70 (m, 2H), 1.26 (m, 19H), 0.89–0.86 (t, 3H);  $^{13}\text{C}$  NMR (100 MHz,  $\text{CDCl}_3$ , TMS)  $\delta$  ppm: 164.27, 163.30, 132.99, 131.61, 127.75, 126.96, 125.86, 117.42, 115.61, 112.65, 41.59, 40.51, 39.99, 31.90, 29.61, 29.32, 27.93, 26.98, 22.67, 14.06; ESI-MS  $m/z$  -ve mode, (%): 605  $[\text{M}-1]^+$ ; Elem. anal.: calculated: C: 71.27%; H: 6.31%; N: 9.23%; Found: C: 68.47%; H: 6.06%; N: 7.53%.

### Spectroscopic Data of Compound NDI-3

MP: 270 °C; FT-IR (KBr,  $\text{cm}^{-1}$ ): 3413, 3280, 2917, 2233, 1702, and 1657;  $^1\text{H}$  NMR (500 MHz,  $\text{CDCl}_3$ , TMS)  $\delta$  ppm: 8.84–8.80 (m, 4H,  $J=7.62$  Hz), 7.80 (s, 4H), 7.60 (brs, 1H), 4.62–4.60 (t, 2H,  $J=5.18$  Hz), 4.23–4.19 (t, 2H,  $J=7.62$  Hz), 4.00–3.38 (t, 2H), 1.73 (m, 2H), 1.25 (m, 26H), 0.88–0.86 (t, 3H);  $^{13}\text{C}$  NMR (100 MHz,  $\text{CDCl}_3$ , TMS)  $\delta$  ppm: 164.25, 163.27, 136.77, 132.96, 131.59, 131.88, 127.75, 126.95, 125.84, 118.62, 115.79, 112.96, 110.13, 41.57, 40.48, 39.98, 31.91, 29.68, 29.24, 27.94, 26.99, 22.68, 14.06; ESI-MS  $m/z$  [%, -ve mode]: 662  $[\text{M}]^+$ ; Elem. anal.: Calculated: C: 72.48%; H: 7.00%; N: 8.45%; found C: 70.32%; H: 6.97%; N: 8.36%.

### Synthesis of NDI-4

NDA (0.5 g, 0.0018 mol) and 4-amino benzonitrile (1.2 equiv) were added to a 50 mL round-bottom flask containing dry DMF (15 mL), which was refluxed until a clear solution was obtained; then, aliphatic amine (1.0 equiv) was added to the reaction mixture and refluxed for a further 12 h under a  $\text{N}_2$  atmosphere. Completion of the reaction was monitored by TLC, following which the reaction mixture was cooled at room temperature to yield a solid, which was filtered and the residue was washed with MeOH to get the crude product. This was further purified by column chromatography using DCM/hexane (95:5, v/v) as the eluent to obtain a pure white solid NDI-4 (0.39 g) in 46% yield.

For the synthesis of NDI-5 and NDI-6, the same experimental procedure described for the preparation of NDI-4 was employed.

### Spectroscopic Data of Compound NDI-4

MP: 275 °C; FT-IR (KBr,  $\text{cm}^{-1}$ ): 2921, 2232, 1706, 1661;  $^1\text{H}$ -NMR (500 MHz,  $\text{CDCl}_3$ , TMS)  $\delta$  ppm: 8.81 (s, 4H), 7.89–7.87 (d, 2H,  $J=8.54$  Hz), 7.49–7.48 (d, 2H,  $J=8.54$  Hz), 4.22–4.19 (t, 2H), 1.79–1.73 (m, 2H), 1.25 (m, 10H), 0.89–0.86 (t, 3H);  $^{13}\text{C}$  NMR (75 MHz,  $\text{CDCl}_3$ , TMS)  $\delta$  ppm: 162.56, 133.29, 131.57, 130.99, 129.86, 127.24, 126.05, 117.96, 113.22, 41.07, 31.73, 29.64, 29.11, 28.01, 27.02, 22.57, 14.08; ESI-MS  $m/z$  (%): 480  $[\text{M}+\text{H}]^+$ ; Elem. anal.: Calculated: C: 72.64%; H: 5.25%; N: 8.76%; Found: C: 72.35%; H: 5.69%; N: 8.10%.

### Spectroscopic Data of Compound NDI-5

MP: 290 °C; FT-IR (KBr,  $\text{cm}^{-1}$ ): 2920, 2228, 1703, 1660;  $^1\text{H}$ -NMR (300 MHz,  $\text{CDCl}_3$ , TMS)  $\delta$  ppm: 8.82 (s, 4H), 7.90–7.87 (d, 2H,  $J=8.39$  Hz), 7.50–7.47 (d, 2H,  $J=8.39$  Hz), 4.23–4.18 (t, 2H), 1.80–1.71 (m, 2H), 1.25 (m, 19H), 0.90–0.85 (t, 3H);  $^{13}\text{C}$  NMR (75 MHz,  $\text{CDCl}_3$ , TMS)  $\delta$  ppm: 162.25, 131.61, 133.30, 131.02, 129.89, 127.32, 126.11, 117.96, 113.28, 41.12, 31.90, 29.67, 29.30, 28.06, 27.07, 22.66, 14.09; ESI-MS  $m/z$  (%): 535  $[\text{M}^+]^+$ ; Elem. anal.: Calculated: C: 76.38%; H: 6.41%; N: 5.24%; Found C: 72.56%; H: 6.23%; N: 8.19%.

### Spectroscopic Data of Compound NDI-6

MP: 265 °C; FT-IR (KBr,  $\text{cm}^{-1}$ ): 2919, 2225, 1703, 1661;  $^1\text{H}$ -NMR (300 MHz,  $\text{CDCl}_3$ , TMS)  $\delta$  ppm: 8.81 (s, 4H), 7.89–7.87 (d, 2H,  $J=8.39$  Hz), 7.49–7.47 (d, 2H,  $J=8.39$  Hz), 4.22–4.19 (t, 2H), 1.79–1.73 (m, 2H), 1.25 (m, 26H), 0.89–0.86 (t, 3H);  $^{13}\text{C}$  NMR (75 MHz,  $\text{CDCl}_3$ , TMS)  $\delta$  ppm: 162.53, 133.30, 131.61, 131.02, 129.86, 117.96, 113.25, 41.10, 31.88, 29.63, 29.32, 27.02, 22.6690, 14.08; ESI-MS  $m/z$  (%): 590  $[\text{M}^+]^+$ ; Elem. anal.: Calculated: C: 75.10%; H: 6.98%; N: 5.24%; Found C: 73.04%; H: 7.04%; N: 6.44%.

## UV/Vis Absorption Spectral Measurements

UV/Vis spectra were recorded by using a Shimadzu UV-1800 spectrophotometer at room temperature. UV/Vis experiments were run in a 3 mL quartz cuvette.

## Film Preparation for UV/Vis Measurements

For recording solid-state UV/Vis spectra of thin films, the solution was drop-cast onto a glass substrate and allowed to dry for 5 mins under high vacuum at 40 °C prior to the measurements. The film thickness was varied by changing the concentration of the solution.

## Fluorescence Measurements

All fluorescence emission experiments were measured in a quartz cell with a 1 cm path length and 355 nm excitation wavelength.

## Film Preparation for Fluorescence Measurements

For recording solid-state fluorescence emission spectra of thin films, solutions of the NDI derivatives  $1 \times 10^{-5}$  M were prepared in THF. The solution was drop-cast onto a quartz substrate and allowed to dry for 5 mins under high vacuum at 40 °C prior to the measurements.

## CV Experiments

Cyclic voltammograms of NDI-1 to NDI-6 amphiphiles in THF ( $1 \times 10^{-5}$  M) were recorded under nitrogen atmosphere with a scan rate of  $50 \text{ mV s}^{-1}$ , 0.1 M  $\text{Bu}_4\text{NHClO}_4$  supporting electrolyte, a Pt disk working electrode, a Pt wire counter electrode, and a saturated calomel reference electrode.

## DSC

The phase-transition temperatures and associated enthalpies were recorded on a PerkinElmer Pyris-1 differential scanning calorimetry system with a heating/cooling rate of  $5^\circ\text{C min}^{-1}$ .

## POM

The LC properties were observed and characterized by using POM (Nikon optiphot-2- pol microscope attached to a hot and cold stage HCS402, with an STC200 temperature controller configured for HCS402 from INSTEC Inc. USA).

## Acknowledgements

S.V.B. (IICT) is grateful for financial support from SERB (Project Code: SB/S1/IC-09/2014), New Delhi, India. N.V.G. acknowledges financial support from CSIR, New Delhi for SRF fellowship. S.V.B. (RMIT) acknowledges financial support from the Australian Research Council under a Future Fellowship Scheme (FT110100152). R.S.B acknowledges financial support from CSIR, New Delhi under the SRA Scheme [13(8772)-A]/2015-Pool].

## Conflict of Interest

The authors declare no conflict of interest.

**Keywords:** alkyl chains · amide hydrogen bonding · liquid crystals · naphthalenediimide · polar headgroup

- [1] Q. Zheng, J. Huang, A. Sarjeant, H. E. Katz, *J. Am. Chem. Soc.* **2008**, *130*, 14410–14410.
- [2] J. C. Maunoury, J. R. Howse, M. L. Turner, *Adv. Mater.* **2007**, *19*, 805–809.
- [3] J. B. Bodapati, H. Icil, *Dyes Pigm.* **2008**, *79*, 224–235.
- [4] S. Sergeyev, W. Pisula, Y. H. Geerts, *Chem. Soc. Rev.* **2007**, *36*, 1902–1929.
- [5] D. D. Sarkar, R. Deb, N. Chakraborty, V. S. N. Rao, *Liq. Cryst.* **2012**, *39*, 1003–1010.
- [6] E. J. Osburn, A. Schmidt, L. K. Chau, S. Y. Chen, P. Smolenyak, N. R. Armstrong, D. F. O'Brian, *Adv. Mater.* **1996**, *8*, 926.
- [7] M. Eich, J. H. Wendorff, *Mikromol. Chem. Rapid Commun.* **1987**, *8*, 59–63.
- [8] C. Röger, F. Würthner, *J. Org. Chem.* **2007**, *72*, 8070–8075.
- [9] M. Al Kobaisi, S. V. Bhosale, K. Latham, A. M. Raynor, S. V. Bhosale, *Chem. Rev.* **2016**, *116*, 11685–11796.
- [10] S. V. Bhosale, C. H. Jani, S. J. Langford, *Chem. Soc. Rev.* **2008**, *37*, 331–342.
- [11] M. Tomasulo, D. M. Naistat, A. J. P. White, D. J. Williams, F. M. Raymo, *Tetrahedron Lett.* **2005**, *46*, 5695–5883.
- [12] G. D. Pantoş, J. L. Wietor, J. K. M. Sanders, *Angew. Chem. Int. Ed.* **2007**, *46*, 2238–2240; *Angew. Chem.* **2007**, *119*, 2288–2290.
- [13] H. Shao, T. Nguyen, N. C. Romano, D. A. Modarelli, J. R. Parquette, *J. Am. Chem. Soc.* **2009**, *131*, 16374–16376.
- [14] R. S. Bhosale, M. Al Kobaisi, S. V. Bhosale, S. Bhargava, S. V. Bhosale, *Sci. Rep.* **2015**, *5*, 14609.
- [15] M. B. Avinash, T. Govindaraju, *Nanoscale* **2011**, *3*, 2536–2543.
- [16] S. P. Goskulwad, D. D. La, R. S. Bhosale, M. Al Kobaisi, S. V. Bhosale, S. V. Bhosale, *RSC Adv.* **2016**, *6*, 39392–39392.
- [17] N. V. Ghule, D. D. La, R. S. Bhosale, M. Al Kobaisi, A. M. Raynor, S. V. Bhosale, S. V. Bhosale, *ChemistryOpen* **2016**, *5*, 157–163.
- [18] K. P. Nandre, S. V. Bhosale, K. V. S. Rama Krishna, A. Gupta, S. V. Bhosale, *Chem. Commun.* **2013**, *49*, 5444–5446.
- [19] Th. Fischer, L. Lasker, J. Stumpe, S. G. Kostromin, *J. Photochem. Photobiol. A* **1994**, *80*, 453–455.
- [20] B. A. Gregg, Y. I. Kim, *J. Phys. Chem.* **1994**, *98*, 2412–2417.
- [21] H. R. Kricheldorf, V. Linker, *Polymer* **1995**, *36*, 1893–1902.
- [22] F. Würthner, M. Stolte, *Chem. Commun.* **2011**, *47*, 5109–5115.
- [23] Zh. Yuan, J. Li, Y. Xiao, Zh. Li, X. Qian, *J. Org. Chem.* **2010**, *75*, 3007.
- [24] P. Gawrys, D. Djurado, J. Rimarcik, A. Kornet, D. Boudinet, V. Lukes, I. Wielgus, M. Zagorska, A. Pron, *J. Phys. Chem. B* **2010**, *114*, 1803–1809.
- [25] Y. Ofir, A. Zelichenok, Sh. Yitzchaik, *J. Mater. Chem.* **2006**, *16*, 2142–2149.
- [26] E. Schab-Balcerzak, A. Iwan, M. Krompiec, M. Siwy, D. Tapa, A. Sikora, M. Palewicz, *Synth. Met.* **2010**, *160*, 2208–2218.
- [27] A. G. Bé, C. Tran, R. Sechrist, J. J. Reczek, *Org. Lett.* **2015**, *17*, 4834–4837.
- [28] Y. Xiao, S. Xiaolu, L. S. Vargas, E. Lacaze, B. Heinrich, B. Donnio, D. Kreher, F. Mathevet, A. J. Attias, *Cryst. Eng.* **2016**, *18*, 4787–4798.
- [29] F. Billeci, F. D'Anna, S. Marullo, R. Noto, *RSC Adv.* **2016**, *6*, 59502–59512.
- [30] W. Lee, C. Lee, H. Yu, D.-J. Kim, C. Wang, H. Y. Woo, J. H. Oh, B. J. Kim, *Adv. Funct. Mater.* **2016**, *26*, 1543–1553.
- [31] K. Upadhyaya, V. Gude, M. Golam, V. S. N. Rao, *Beilstein J. Org. Chem.* **2013**, *9*, 26–35.
- [32] R. A. Cormier, B. A. Gregg, *Chem. Mater.* **1998**, *10*, 1309–1319.
- [33] M. Jayakannan, P. Deepa, K. Divya, *J. Polym. Sci. Part A Polym. Chem.* **2006**, *44*, 42–52.

Received: September 12, 2017

Version of record online November 15, 2017